TIME SIGNATURES OF IMPULSIVELY GENERATED WAVES IN A CORONAL PLASMA

K. MURAWSKI* and B. ROBERTS
Department of Mathematical and Computational Sciences, University of St Andrews, Fife KY16 9SS, Scotland

(Received 20 August, 1993, in revised form 25 January, 1994)

Abstract. Impulsively generated waves in solar coronal loops are numerically simulated in the framework of cold magnetohydrodynamics. Coronal inhomogeneities are approximated by gas density slabs embedded in a uniform magnetic field. The simulations show that an initially excited pulse results in the propagation of wave packets which correspond to both trapped and leaky waves. Whereas the leaky waves propagate outside the slab, the trapped waves occur as a result of a total reflection from the slab walls. Time signatures of these waves are made by a detection of the trapped waves at a fixed spatial location. For waves excited within the slab, time signatures exhibit periodic, quasi-periodic and decay phases. The time signatures for waves excited outside the slab, or for a multi-series of variously shaped impulses generated at different places and times, can possess extended quasi-periodic phases. The case of parallel slabs, when the presence of a second slab influences the character of wave propagation in the first slab, exhibits complex time signatures as a result of solitary waves interaction.

1. Introduction

The localized and complex nature of mass density in the solar corona (e.g., Golub, 1990; Shibata *et al.*, 1992) and dynamical effects, either observed in form of pulsating radio emission, or theoretical requirements of coronal heating has lead to extensive investigations of the behaviour of waves in coronal loops (e.g., Roberts, Edwin, and Benz, 1984; Aschwanden, 1987; Pasachoff, 1990; Zlobec *et al.*, 1992). The behaviour of MHD waves in such structures is not fully explored (see, however, Hollweg and Roberts 1984; Berton and Heyvaerts 1987; and Ruderman 1992). Among a variety of different structures the case of two parallel loops is of interest because the presence of one loop has an influence on wave propagation in the other loop. See, for example, Tajima *et al.* (1987) for periodic oscillations found in two coalescing loops driven by current loop coalescence. It is natural, then, to enquire into the detailed nature of the waves propagating along two parallel loops. Such an enquiry has perhaps an intrinsic importance as the waves are generally believed to form the basis (Roberts, Edwin, and Benz, 1984) for a possible explanation of the long-standing puzzle of short ($\sim$1 s) pulsations studied in Type IV coronal radio events (e.g., Tapping, 1978; Krüger, 1979; Trottet *et al.*, 1981; Aschwanden, 1987).

* Present address: Center for Plasma Astrophysics, Katholieke Universiteit Leuven, B-3001 Leuven, Belgium.

Solar Physics **151:** 305–317, 1994.

An understanding of coronal waves is also of central importance for the question of coronal heating (e.g., Hollweg, 1990; Goossens, 1991).

Roberts, Edwin, and Benz (1983, 1984) studied impulsively generated waves in coronal loops which were represented by density enhancements. The theory developed by Roberts, Edwin, and Benz has been compared with the results of numerical experiments in Murawski and Roberts (1993a, b) and Murawski and Goossens (1994). Both the linear and nonlinear MHD systems have been solved, and are in general agreement with the analytical predictions of linear theory. The numerical simulations have been performed for an isolated slab with the waves excited on the axis of the slab.

For the typical coronal conditions the Alfvén speed V_A and the sound speed c_s are of the order of 10^3 km s^{-1} and 200 km s^{-1}, respectively, and so give a low plasma $\beta = p/(B^2/2\mu) = \frac{1}{2}\gamma c_s^2/V_A^2 (\simeq 1/25)$. Thus the solar corona is magnetically dominated. Consequently, it is of interest to consider a cold ($\beta = 0$) plasma, neglecting the effects of gas pressure. We also neglect gravity. We assume that motions are polarized in the xz-plane of a Cartesian coordinate system and are independent of y. This simple model of a coronal loop has been described in greater detail by Murawski and Roberts (1993a, b). More realistic model including curvature and current-carrying coronal loops has been used recently by Cargill, Chen, and Garren (1993).

The purpose of this paper is to investigate numerically impulsively generated waves in slab density enhancements representative of coronal conditions, extending the analysis of Murawski and Roberts (1993a, b). We are particularly interested in the time scales associated with the impulsive waves which arise when generated at an off-axis location in the slab. The phenomenon of cross-talk between waves excited in two parallel slabs is of special interest (see also Murawski, 1993) and we determine the time signatures associated with the waves.

2. Numerical Results

In this part of the paper we present results of the numerical simulations for two cases: an isolated dense slab, and two parallel slabs. Linear motions of the isolated slab are investigated by solving numerically the two dimensional wave equation for the magnetic potential (flux function) $A(x, z, t)$, the perturbed magnetic field being $\mathbf{B} = (-\partial A/\partial z,\ 0,\ \partial A/\partial x)$; see also Murawski and Roberts (1993a). The linear wave equation is solved by the fast Fourier transform method in space and the second-order Runge–Kutta method in time (see Murawski and Roberts (1993a) for a description of the numerical algorithm). The case of two parallel slabs is investigated nonlinearly, the nonlinear set of equations being solved by an application of a flux conserving code (Murawski and Goossens, 1994).

Illustrations of our numerical results are given for an Alfvén speed V_A inside the slab of 10^3 km s^{-1} and a slab width of $2a = 1500$ km s^{-1}.

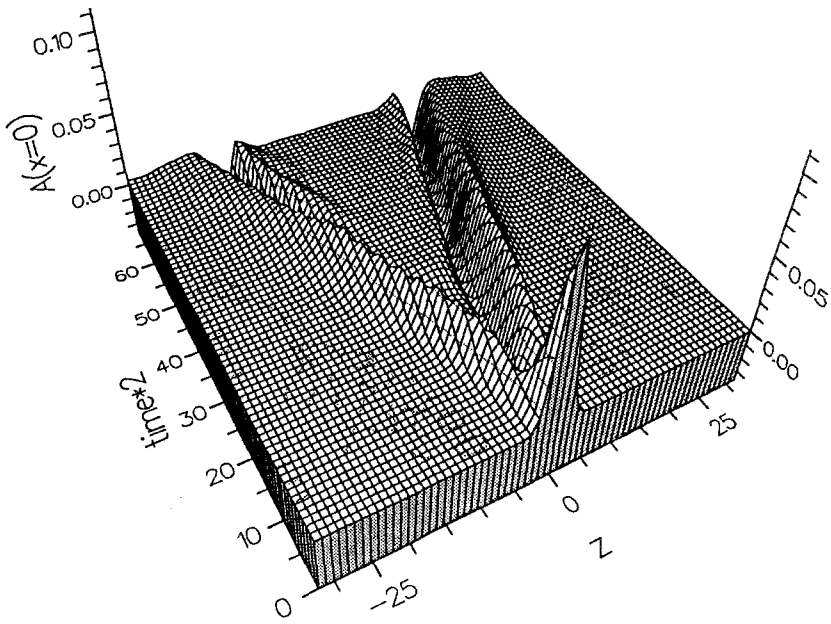

Fig. 1. The magnetic potential $A(x = 0, z, t)$ as a function of time and the distance from the source of the initial profile excited at $x = z = 0$. The initial profile has indices $m = n = 2$ (see Equation (2.1)). The time is in units of the Alfvén transit time, a/V_A, and distance is in units of the slab half-width a. Notice a transition at $z \simeq 15a$ and $t \simeq 25a/V_A$, where the largest amplitude hump flattens out to be replaced by a valley.

2.1. THE ISOLATED SLAB

We consider the behaviour of impulsively generated linear waves, taking an initial pulse of the form

$$A(x,\, z,\, t = 0) = A_0 \operatorname{sech}^m\left(\frac{x - x_0}{a}\right) \operatorname{sech}^n\left(\frac{z - z_0}{a}\right). \tag{2.1}$$

Here A_0 is the amplitude of the initial magnetic potential A which is centred around the point (x_0, z_0). We consider various choices for the source location (x_0, z_0) and also for the indices m and n. The magnetic slab has an equilibrium gas density given by (see also Murawski and Roberts, 1993a)

$$\rho_0(x) = \begin{cases} \rho_0, & |x| \le a \\ \rho_e + (\rho_0 - \rho_e) \operatorname{sech}^N\left(\dfrac{|x| - a}{a}\right), & |x| > a, \end{cases} \tag{2.2}$$

the power N being chosen to obtain a gas density in the form of a top-hat profile but with its edges smoothed. We take $N = 14$ throughout to obtain an almost rectangular shape.

Consider first the case of an initially symmetric disturbance located at the centre of the density inhomogeneity, so that $x_0 = z_0 = 0$. We take a density ratio of $\rho_0/\rho_e = 5$, and an initial pulse with $m = n = 2$. The initial pulse disperses in the xz-plane with clearly distinguishable trapped perturbations propagating along the slab. Murawski and Roberts (1993a) discuss this process in detail. Figure 1 shows such perturbations along the slab axis ($x = 0$) as a function of the time t and the coordinate z. As expected, two wave fronts are created by the initial pulse and propagate in opposite directions. Time signatures corresponding to the behaviour of the potential $A(x, z, t)$ are calculated on the slab axis ($x = 0$) at a distance $z = z^*$ from the source at $z = 0$. A clear transition in the form of the time signatures occurs at the point $z^* \simeq 15a$, where a hump considerably flattens to be replaced by a valley. This occurs at a time $t \simeq 25a/V_A$. The time signature made at a specific z^* may be constructed from Figure 1. It is similar to that shown in Figure 3 of Murawski and Roberts (1993a), which presents the behaviour of the potential A calculated at the point $x = 0$, $z = z^* = 8a$. The three phases determined analytically by Roberts, Edwin, and Benz (1983, 1984) can be distinguished. The quasi-periodic phase begins abruptly with a large hump and a valley following it and small amplitude disturbances within it. Such a sudden onset of the quasi-periodic phase is somewhat reminiscent of the pulsation event reported in radio emission by McLean *et al.* (1971) and McLean and Sheridan (1973).

A less abrupt transition from the periodic phase (visible as weak oscillations for times $t < 11a/V_A$ in Figure 2(b)) to the quasi-periodic phase (after $t > 11a/V_A$) occurs in the case of a steeper initial profile. For example, Figure 2 shows the time signatures for steeper pulses, taking $m = n = 4$ in Figure 2(a) and $m = n = 6$ in Figure 2(b). The initial pulses are excited at the slab centre, so $x_0 = z_0 = 0$. The periodic phase, represented in Figure 3 of Murawski and Roberts (1993a) by a straight horizontal line, is here more pronounced with small amplitude oscillations within it. The periodic phase occurs for $t \leq 8a/V_A$. Steeper initial pulses also lead to more structured quasi-periodic phases, with shorter lasting largest humps and an increase in the number of oscillations. Four main oscillations appear in Figure 2(a), and five oscillations are in Figure 2(b). As a consequence, time scales associated with a single pulse are smaller for steeper initial profiles. For example, in Figure 2(b) they are about 2 s, half those in Figure 2(a). For the case of steep profiles, the quasi-periodic phases lasts longer; for example, in Figure 2(b), where $m = n = 6$, the quasi-periodic phase lasts about $\tau_d \simeq 30a/V_A (\approx 20$ s) and it is more distinctive than is the case of Figure 2(a).

Quite different time signatures characterize waves which are generated by an impulse located *outside* the slab. We consider the case of a pulse with $m = n = 2$ initially launched at $x = x_0$, $z = z_0 = 0$. The slab has a density ratio of $\rho_0/\rho_e = 5$. The time-dependence of the potential A exhibits an extended quasi-periodic phase, the duration of which increases with increasing x_0. See Figure 3. Moreover, the quasi-periodic phase becomes more structured with increasing x_0: for $x_0 = a/2$ (Figure 3(a)) it is similar to the quasi-periodic phase of the $x_0 = 0$ case (cf.

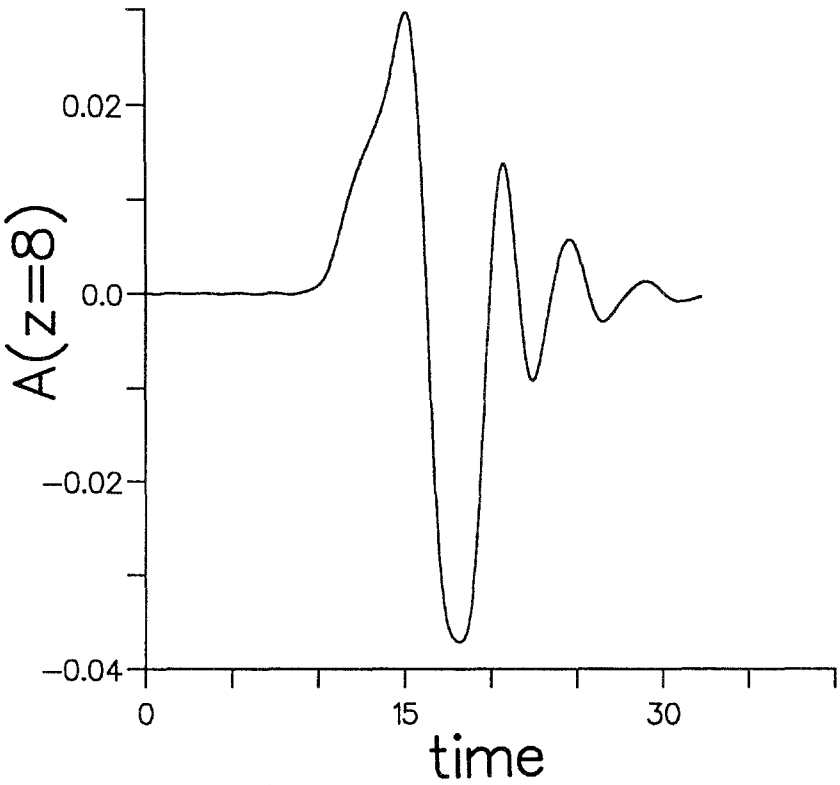

Fig. 2a.

Fig. 2. The time signature of $A(x = 0, z = 8a)$ for waves impulsively generated (at $x = z = 0$) in a slab with $\rho_0/\rho_e = 5$, taking (a) $m = n = 4$, and (b) $m = n = 6$. Notice the shorter time scales and longer-lasting quasi-periodic phase associated with the steeper initial profiles.

Figure 3 of Murawski and Roberts 1993a); for $x_0 = 3a$ the duration time of the quasi-periodic phase is about 15 Alfvén transit times (Figure 3(b)), corresponding to 11-s oscillations. However, the duration time of a single pulse is much shorter and is of order 2 time units (1.5-s oscillations).

2.2. Two parallel slabs

We turn now to the behaviour of fast waves in two parallel coronal slabs, considering their *nonlinear* form. The slabs are located at $x = \pm 2a$. These waves are described by the nonlinear cold plasma equations of ideal MHD (see Equations (2.2)–(2.5) of Murawski and Roberts, 1993b). Specifically, we take

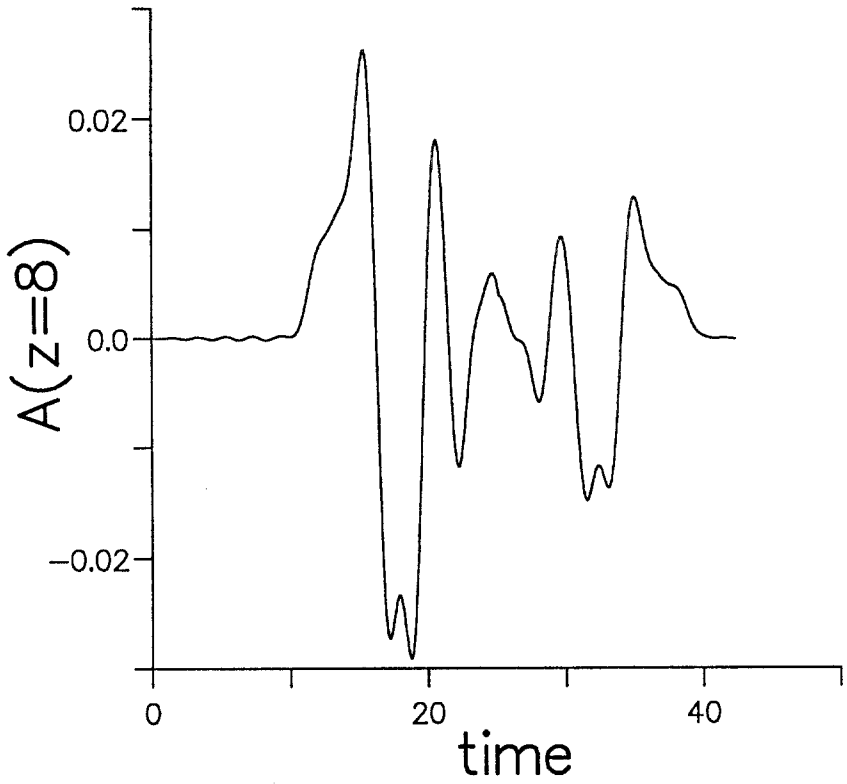

Fig. 2b.

$$\rho_0(x) = \begin{cases} \rho_0, & |x \pm 2a| \leq a, \\ \rho_e + (\rho_0 - \rho_e)\,\mathrm{sech}^{14}\left(\dfrac{|x+2a|-a}{a}\right), & |x+2a| > a, \\ \rho_e + (\rho_0 - \rho_e)\,\mathrm{sech}^{14}\left(\dfrac{|x-2a|-a}{a}\right), & |x-2| > a. \end{cases} \tag{2.3}$$

At $t = 0$ we implement the conditions which represent density, flow and magnetic field:

$$\rho(x, z, t = 0) = \rho_0(x) + \rho_p C(x, z), \tag{2.4}$$

$$V_x(x, z, t = 0) = V_{xp} C(x, z), \tag{2.5}$$

$$V_z(x, z, t = 0) = V_{zp} C(x, z), \tag{2.6}$$

$$B_x(x, z, t = 0) = -2B_p C(x, z)\,\tanh\left(\frac{z}{a}\right), \tag{2.7}$$

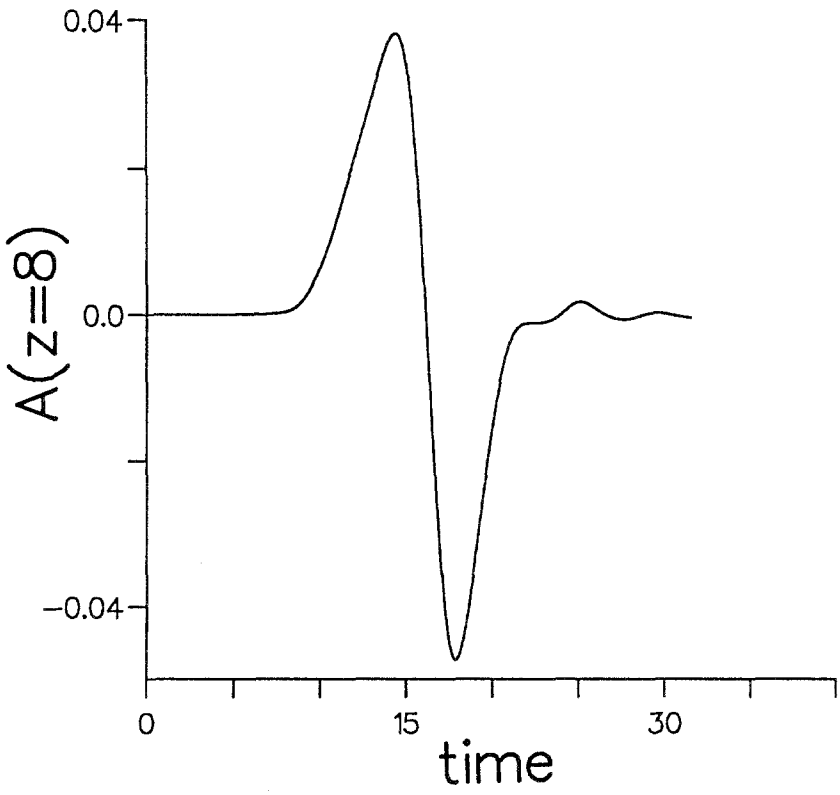

Fig. 3a.

Fig. 3. The time signature of disturbances with $m = n = 2$ that are impulsively generated at an off-axis position: (a) $x_0 = a/2$, (b) $x_0 = 3a$. The density ratio $\rho_0/\rho_e = 5$ and $z_0 = 0$. A more complicated and longer lasting quasi-periodic phase characterizes the time signatures in the case of (b).

$$B_z(x, z, t = 0) = B_0 + 2B_p C(x, z) \tanh\left(\frac{x - 2a}{a}\right), \tag{2.8}$$

where $C(x, z) = \operatorname{sech}^2((x - 2a)/a) \operatorname{sech}^2(z/a)$. Wave profiles which correspond to these perturbations are shown in Figure 4.

As in the case of an isolated slab, the time evolution of the perpendicular velocity V_x occurs on the scale of a few Alfvén transit times, a/V_A. The initially symmetric profile (2.5) evolves to become asymmetric as the wave feels the gradient in Alfvén speed, low inside the slabs and larger outside them. These gradients permit total reflection and the occurrence of trapped waves, which propagate initially along the right-hand slab. As a consequence of the nonlinearity, the hump which propagates in the negative z-direction is larger than the hump propagating in the z-direction. Because of the gradient in Alfvén speed, these humps propagate slower than the outwardly propagating ripples. The ripples leak energy from the right-hand slab, leading to oscillations in the left-hand slab. Some of the oscillations entering the

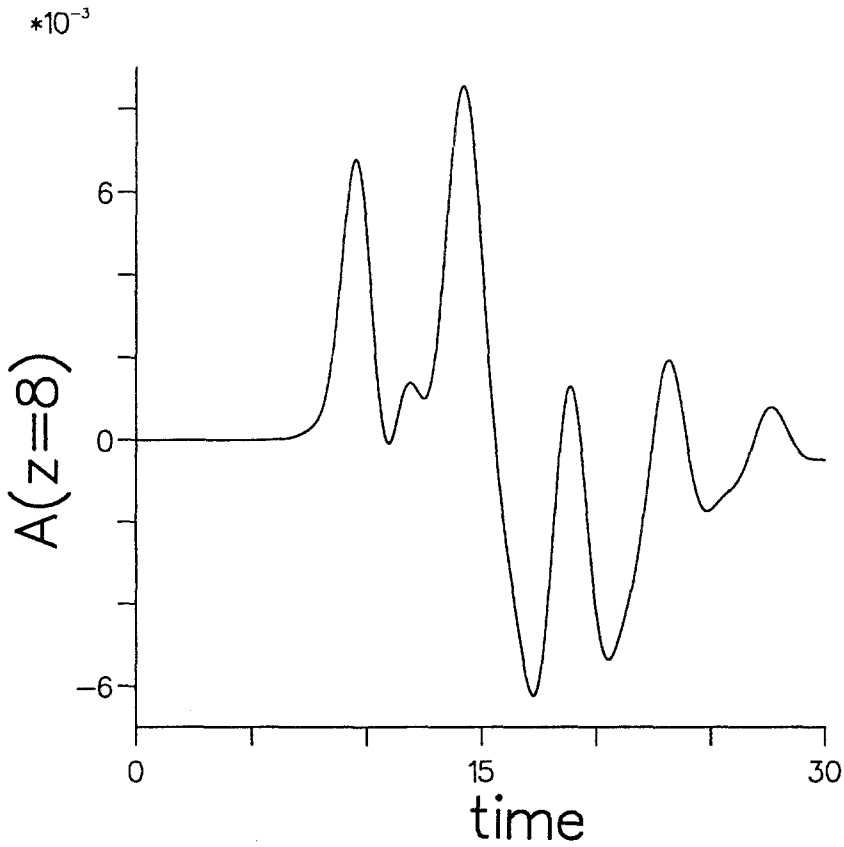

Fig. 3b.

left slab are totally reflected from the walls of the slab, and such reflection creates a hump in the left slab. In the early stages of its time evolution the hump moving in the left-hand slab has a small amplitude (Figure 4(a)) and lags behind the hump moving in the right-hand slab. But with the lapse of time the distance between the two humps decreases and the amplitude of the hump in the left-hand slab grows as the humps interact attractively through their outskirts. This interaction results in energy transfer from the right-hand hump. See Figure 4(b).

Just as with an isolated slab, the trapped waves exhibit time signatures which may be detected by examining the perpendicular velocity V_x at a fixed spatial location. But what effect does a second slab have on those signatures? Figure 5 shows the signals of V_x in two slabs, detected at $z = \pm 8a$. The time signatures are more complicated than in the case of an isolated slab. It is of interest to compare the parallel slabs results, depicted here in Figure 5(a), with Figure 3 of Murawski and Roberts (1993b). The signal in the left-hand slab is represented by a dotted curve, that in the right-hand slab by a solid curve. As a result of wave trapping and an interaction between the two humps, the oscillations in the left slab are smaller in

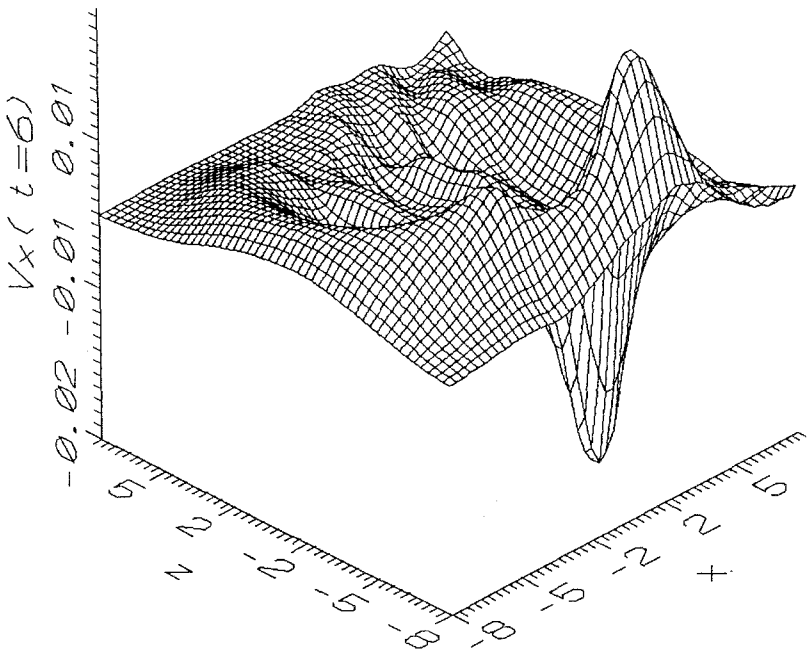

Fig. 4a.

Fig. 4. The spatial variation of the perpendicular velocity V_x for impulsively generated waves which are initially (at $t = 0$) propagating in the right-hand coronal slab. The initial conditions are given by Equations (2.4)–(2.8) with $\rho_p = 0.1\ \rho_0$, $V_{xp} = V_{zp} = 0.05\ V_A$, $B_p = 0.05\ B_0$. The profiles are for times (a) $t = 6\ a/V_A$, (b) $t = 11\ a/V_A$.

amplitude than those in the right slab. As a consequence of the asymmetry in the z-direction, time signatures depend upon the location of the detector. The signature at $z = 8a$ is shown in Figure 5(b). This signal is characterized by complex oscillations which are, however, of small amplitude and thus, from an observational point of view, are probably less important than those seen at $z = -8a$ (Figure 5(a)). The signal is interrupted when wave breaking occurs, evident in the mass density ρ at a time $t \simeq 25\ a/V_A$.

The perpendicular V_x profile can be compared with the corresponding spatial variation of V_x, and reveals greater asymmetry in the wave propagation in the case of two parallel slabs than in the case of an isolated slab (compare Figures 5(a) and 5(b)) here with Figures 2(b) and 2(c)) of Murawski and Roberts (1993b) and Figure 1 of Murawski and Goossens (1994)).

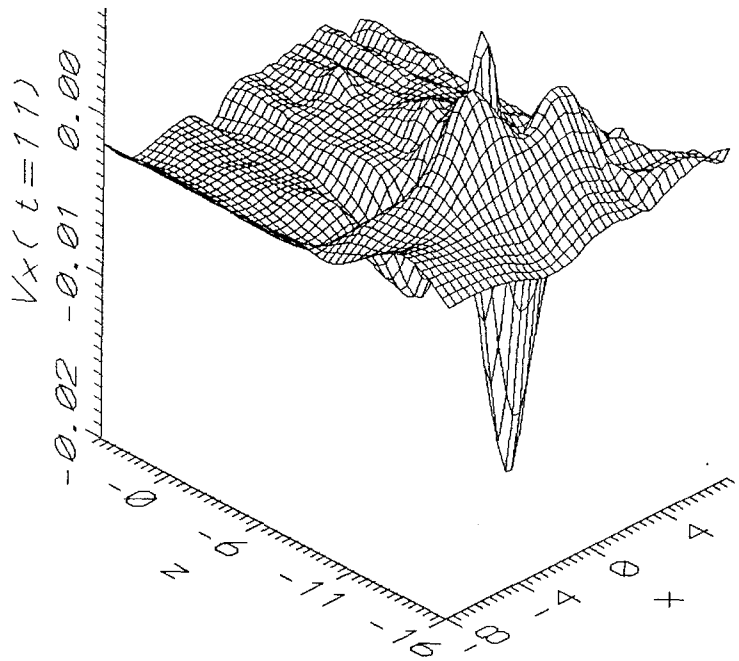

Fig. 4b.

3. Discussion

We have investigated numerically impulsively generated fast waves in smoothed top-hat slabs under coronal conditions. In the simplest case of a single wave source placed on the axis of an isolated slab, such waves possess a distinctive time signature which consists of three phases, a periodic phase followed by a quasi-periodic phase and finally by a decay phase (Roberts, Edwin, and Benz, 1983, 1984). The numerical results presented here show that such time signatures can be more complex for waves excited outside an isolated slab or for the case of a multi-series of impulses generated at different places and times. Waves excited outside the slab lead to extended quasi-periodic phases, as wave trapping occurs for a series of 'modulations' with a circular-like pattern. These modulations move towards the slab, where some of them are reflected and transmitted at the right-hand wall of the slab. Transmitted modulations may then be totally reflected from the left-hand wall and in consequence become trapped by the slab, and so give rise to oscillations in the time signatures. This process is repeated for the next modulation which subsequently approaches the slab. Thus, time signatures are built up by a sequence of oscillations, all originating from the initial pulse.

The character of the time signatures depends on the slab strength (i.e., density

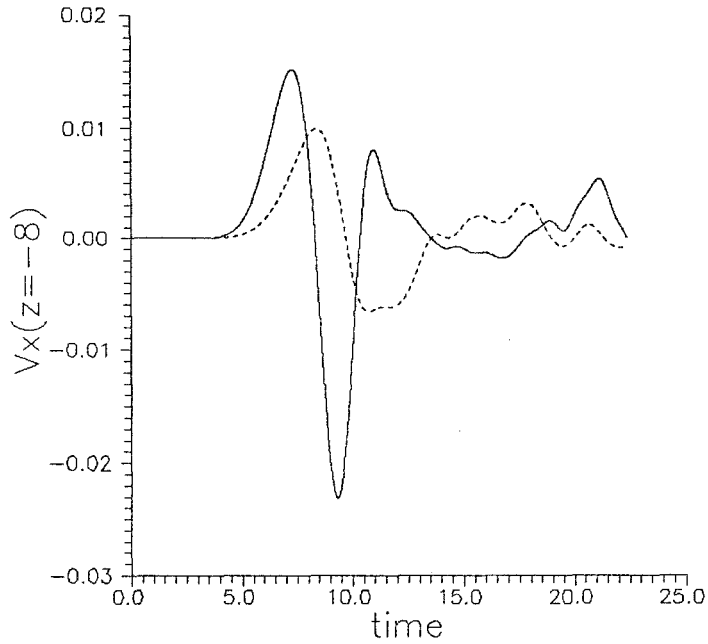

Fig. 5a.

Fig. 5. Time signatures of V_x associated with the impulsively generated waves of Figure 4. The solid line corresponds to the velocity V_x in the right-hand slab, and the broken line is for the left-hand slab. V_x is measured at the symmetric locations (a) $z = -8a$ and (b) $z = 8a$.

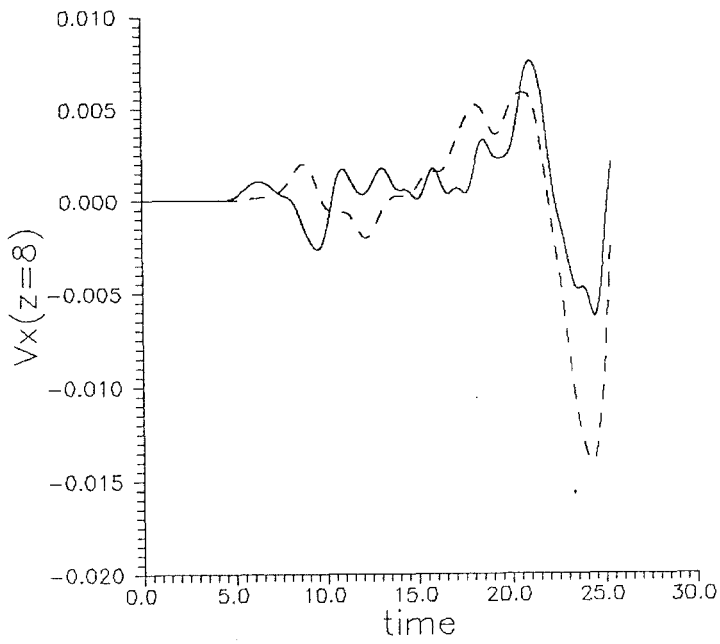

Fig. 5b.

contrast) and its detailed shape. For stronger slabs the duration time of the quasi-periodic phase is longer because the minimum of the group velocity $c_g^{\min}$ is smaller (Roberts, Edwin, and Benz, 1984). A smooth transition from periodic to quasi-periodic waves is observed for the case of increasingly smoother slabs, as the dispersion does not change sign (i.e., $\partial^2\omega/\partial k^2 = c_g \partial c_g/\partial\omega \neq 0$). The time signatures also depend on the distance from the source point (see Figure 1).

It is interesting to note that steeper initial profiles lead to longer lasting quasi-periodic phases. In the case of a wide pulse, a main contribution to the time signature is provided by the hump and valley that follows it. Oscillations following the hump and valley are considerably lower in amplitude. Therefore, we see that the large amplitude phase is short-lived. By contrast, a steep initial profile evolves into a wavy pattern in which a leading hump and a valley are comparable in their amplitudes to the oscillations that follow them, and consequently the larger amplitude phase is extended in time.

The presence of a second slab has direct consequences on the propagation of impulsively generated waves. As a result of energy leakage from one slab, oscillations can enter the second slab. These oscillations are totally reflected in the second slab and wave trapping occurs. The trapped waves in the slab can interact with themselves and consequently the time signatures of such waves are more complicated than in the case of an isolated slab. The numerical results show that these time signatures can also be different if detected at different z-sides of the initial disturbance.

The interaction between trapped humps in two parallel slabs is reminiscent of an elastic interaction between cylindrical solitary waves of the Zakharov–Kuznetsov equation which describes ion-acoustic waves propagation in a magnetic environment (see, for example, Iwasaki, Toh and Kawahara (1990) and Murawski and Edwin (1992)). It is also interesting to note that these humps are very robust both with respect to numerical noise and to the perturbations which are exerted by leaky waves. This behaviour and the elastic interaction between humps leads us to a supposition that the trapped waves are in fact soliton-like structures. This supposition is supported by the existence of solitons in optical fibers (e.g., Hasegawa, 1989) and the analogy between such fibres and coronal wave guides.

Acknowledgements

K. M. wishes to express his thanks to the SERC for its financial support and to the Onderzoeksfonds K. U. Leuven for awarding him a fellowship and its financial support.

References

Aschwanden, M. J.: 1987, *Solar Phys.* **111**, 113.
Berton, R. and Heyvaerts, J.: 1987, *Solar Phys.* **109**, 201.
Cargill, P. J., Chen, J., and Garren, D. A.: 1993, *Astrophys. J.*, in press.

Golub, L.: 1990, in P. Ulmschneider and E. R. Priest (eds.), *Mechanisms of Chromosphere and Coronal Heating*, Springer-Verlag, Heidelberg, p. 115.
Goossens, M.: 1991, in E. R. Priest and A. W. Hood (eds.), *Advances in Solar System Magnetohydrodynamics*, Cambridge University Press, Cambridge, p. 137.
Hasegawa, A.: 1989, *Optical Solitons in Fibers*, Springer Tracts in Modern Physics, Vol. **116**, Springer-Verlag, Heidelberg.
Hollweg, J. V.: 1990, *Comp. Phys. Rep.* **12**, 205.
Hollweg, J. V. and Roberts, B.: 1984, *J. Geophys. Res.* **89A**, 9703.
Iwasaki, H., Toh, S., and Kawahara, T.: 1990, *Physica* **D43**, 293.
Krüger, A.: 1979, *Introduction to Solar Radio Astronomy and Radio Physics*, D. Reidel Publ. Co., Dordrecht, Holland.
McLean, D. J. and Sheridan, K. V.: 1973, *Solar Phys.* **32**, 485.
McLean, D. J., Sheridan, K. V., Stewart, R. T., and Wild, J. P.: 1971, *Nature* **234**, 140.
Murawski, K.: 1993, *Acta Astron.* **43**, 161.
Murawski, K. and Edwin, P.: 1992, *J. Plasma Phys.* **47**, 75.
Murawski, K. and Goossens, M.: 1994, *J. Geophys. Res.*, submitted.
Murawski, K. and Roberts, B.: 1993a, *Solar Phys.* **144**, 101.
Murawski, K. and Roberts, B.: 1993b, *Solar Phys.* **145**, 145.
Pasachoff, J. M.: 1990, in P. Ulmschneider and E. R. Priest (ed.), *Mechanisms of Chromosphere and Coronal Heating*, Springer-Verlag, Heidelberg, p. 25.
Roberts, B, Edwin, P. M., and Benz, A. O.: 1983, *Nature* **305**, 688.
Roberts, B, Edwin, P. M., and Benz, A. O.: 1984, *Astrophys. J.* **279**, 857.
Ruderman, M. S.: 1992, *J. Geophys. Res.* **97**, 843.
Shibata, K. *et al.*: 1992, *Publ. Astron. Soc. Japan* **44**, L173.
Tajima, T., Sakai, J., Nakajima, H., Kosugi, T., Brunel, F., and Kundu, M. R.: 1987, *Astrophys. J.* **321**, 1031.
Tapping, K. F.: 1978, *Solar Phys.* **59**, 145.
Trottet, G., Kerdraon, A., Benz, A. O., and Treumann, R.: 1981, *Astron. Astrophys.* **93**, 164.
Zlobec, P., Messerotti, M., Dulk, G. A., and Kucera, T.: 1992, *Solar Phys.* **141**, 165.